Quantifying Solvated Electrons' Delocalization

Benjamin G. Janesko, Giovanni Scalmani, and Michael J. Frisch

Physical Chemistry Chemical Physics 2015

Supporting Information document 1 of 3: Figures and tables referenced in the text

SI-I. FULL REF. 48 CITATION:

Gaussian Development Version, Revision H.35, M. J. Frisch, G. W. Trucks, H. B. Schlegel, G. E. Scuseria, M. A. Robb, J. R. Cheeseman, G. Scalmani, V. Barone, B. Mennucci, G. A. Petersson, H. Nakatsuji, M. Caricato, X. Li, H. P. Hratchian, A. F. Izmaylov, J. Bloino, B. G. Janesko, F. Lipparini, G. Zheng, J. L. Sonnenberg, W. Liang, M. Hada, M. Ehara, K. Toyota, R. Fukuda, J. Hasegawa, M. Ishida, T. Nakajima, Y. Honda, O. Kitao, H. Nakai, T. Vreven, J. A. Montgomery, Jr., J. E. Peralta, F. Ogliaro, M. Bearpark, J. J. Heyd, E. Brothers, K. N. Kudin, V. N. Staroverov, T. Keith, R. Kobayashi, J. Normand, K. Raghavachari, A. Rendell, J. C. Burant, S. S. Iyengar, J. Tomasi, M. Cossi, N. Rega, J. M. Millam, M. Klene, J. E. Knox, J. B. Cross, V. Bakken, C. Adamo, J. Jaramillo, R. Gomperts, R. E. Stratmann, O. Yazyev, A. J. Austin, R. Cammi, C. Pomelli, J. W. Ochterski, R. L. Martin, K. Morokuma, V. G. Zakrzewski, G. A. Voth, P. Salvador, J. J. Dannenberg, S. Dapprich, P. V. Parandekar, N. J. Mayhall, A. D. Daniels, O. Farkas, J. B. Foresman, J. V. Ortiz, J. Cioslowski, and D. J. Fox, Gaussian, Inc., Wallingford CT, 2010.

SI-II. MODEL SYSTEMS

.

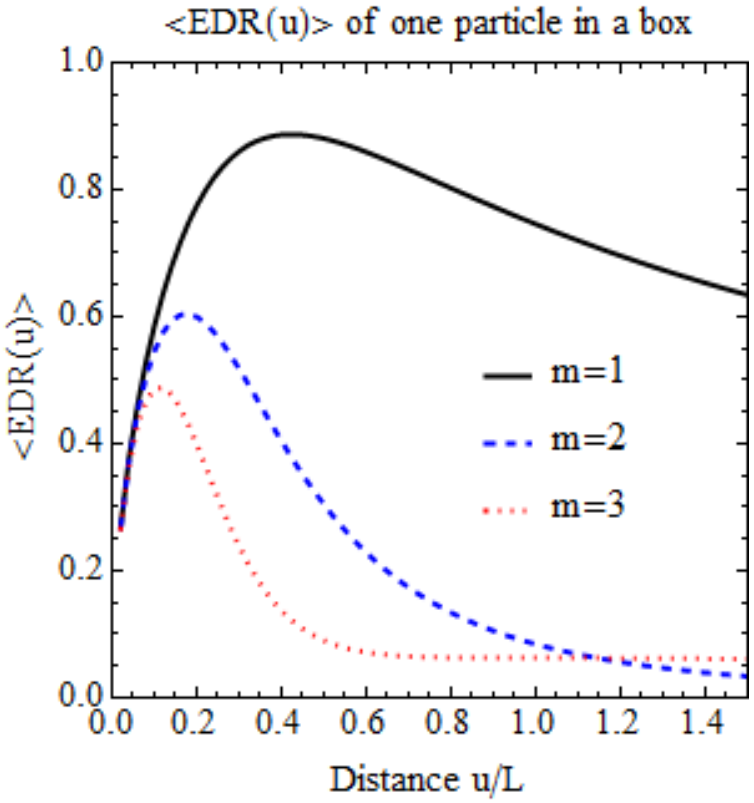

FIG. SI-1: $\langle \mathrm{EDR}(u) \rangle$ for the $m = 1, 2, 3$ states of a single particle in a 1-D box.

SI-III. HYDRATED ELECTRONS

.

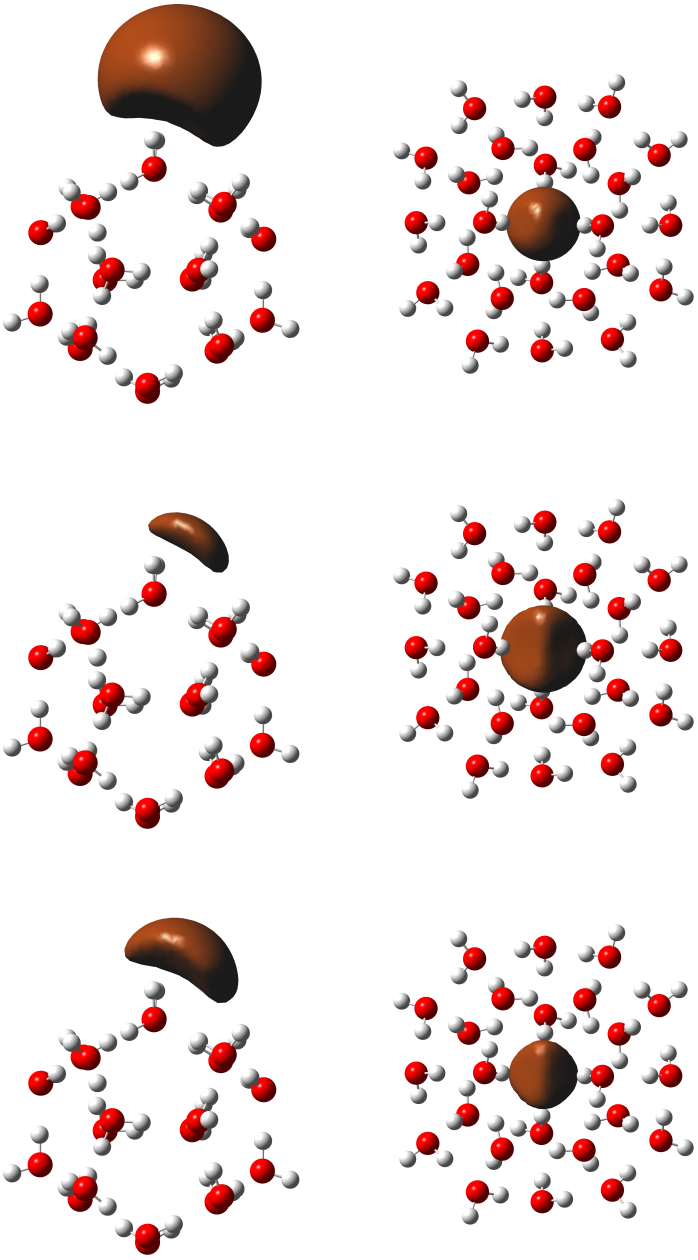

FIG. SI-2: Isosurfaces of EDR($\vec{r}; u_{av}$) for surface state $(H_2O)^-_{20}$ 5^{12} A (left) and cavity state $(H_2O)^-_{24}$ $5^{12}6^2$B (right). Top to bottom are HF, LDA and B3LYP calculations. $(H_2O)^-_{24}$ LDA and B3LYP isosurface 0.75, others use isosurface 0.8.

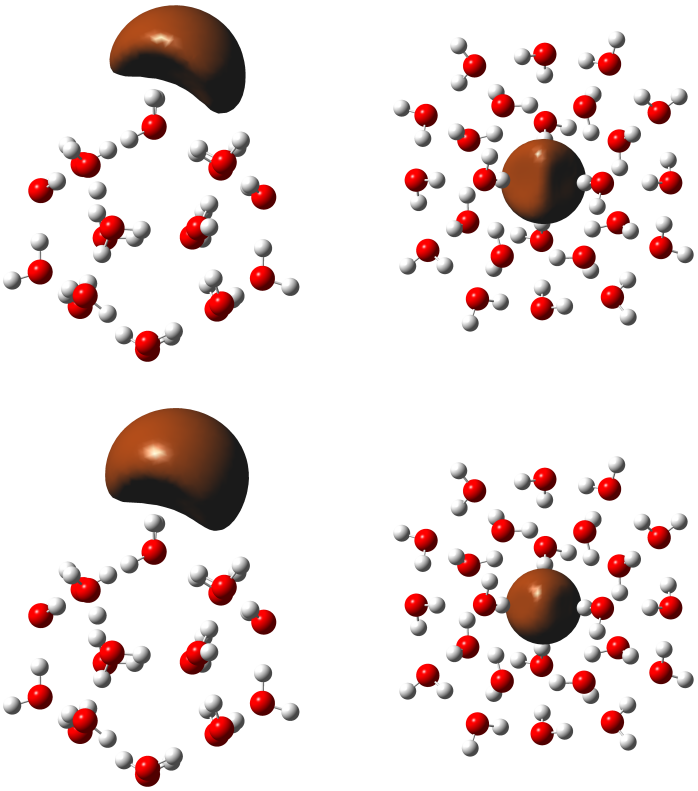

FIG. SI-3: As in Figure SI-2, for BHLYP (top) and LC-ωPBE (bottom) calculations. $(H_2O)_{24}^-$ BHLYP isosurface 0.75, others use isosurface 0.8.

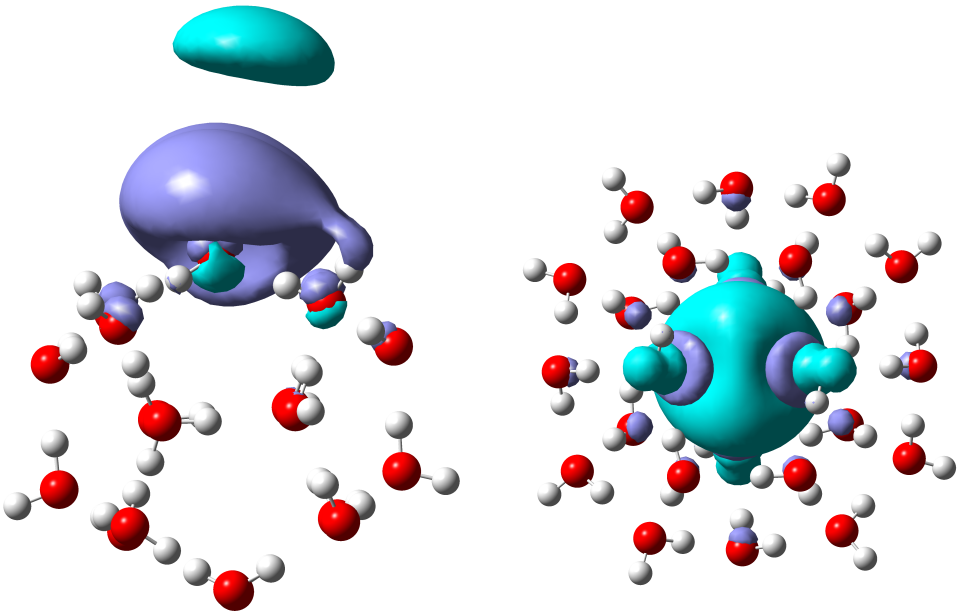

FIG. SI-4: Isosurfaces $|\Delta\rho(\vec{r})| = 0.0001$ bohr^{-3} of the difference between MP2 and Hartree-Fock spin densities for surface state $(H_2O)_{20}^-$ 5^{12} A (left) and cavity state $(H_2O)_{24}^-$ $5^{12}6^2$B (right). Light blue regions are depopulated by electron correlation, darker blue regions are populated by electron correlation.

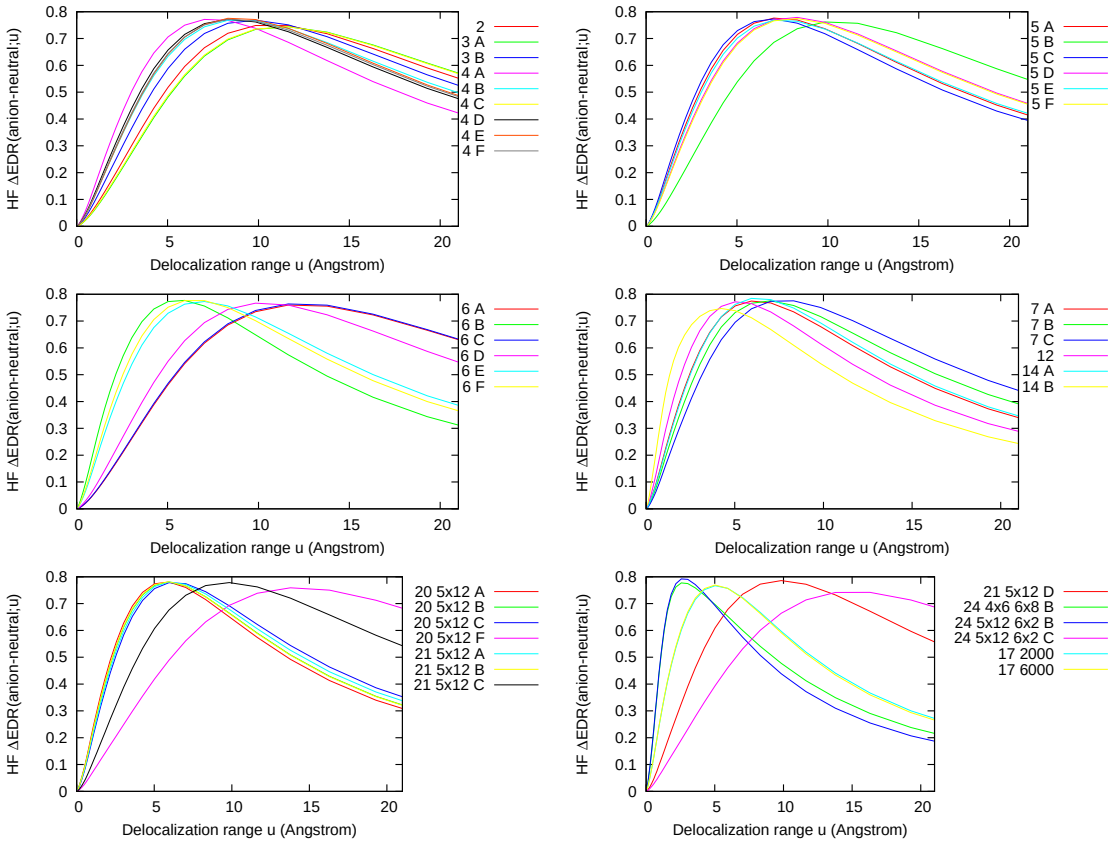

FIG. SI-5: HF ΔEDR(anion-neutral; u) for $(H_2O)_N^-$ clusters

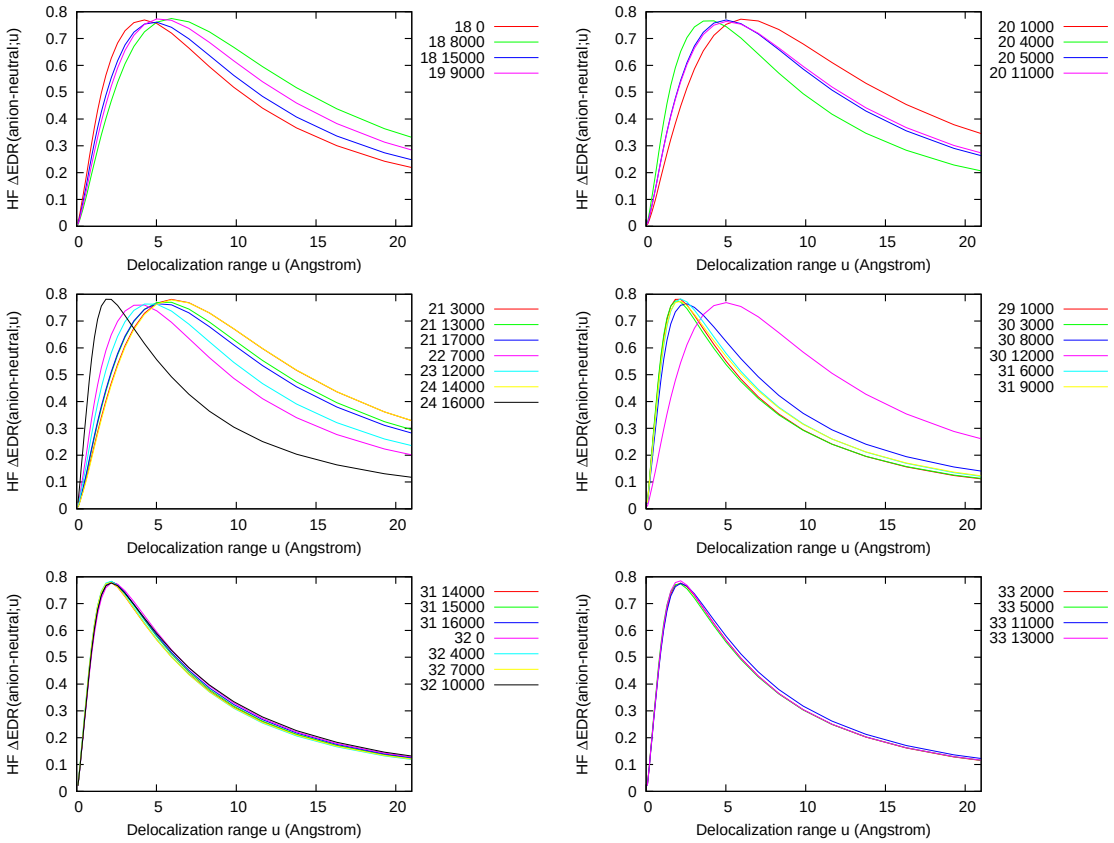

FIG. SI-6: HF ΔEDR(anion-neutral; u) for $(H_2O)_N^-$ clusters

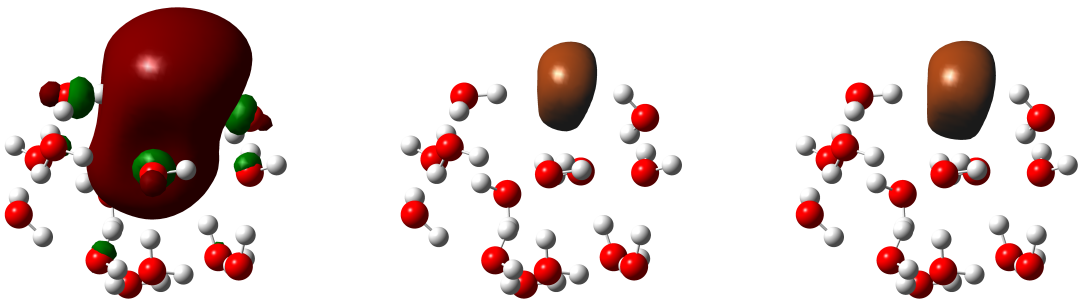

FIG. SI-7: Isosurfaces SOMO=0.002 bohr$^{-3/2}$ (left), and HF (middle) and MP2 (right) EDR(r; u_{av})=0.8, of "cluster" isomer $(H_2O)_{14}^-$ B.

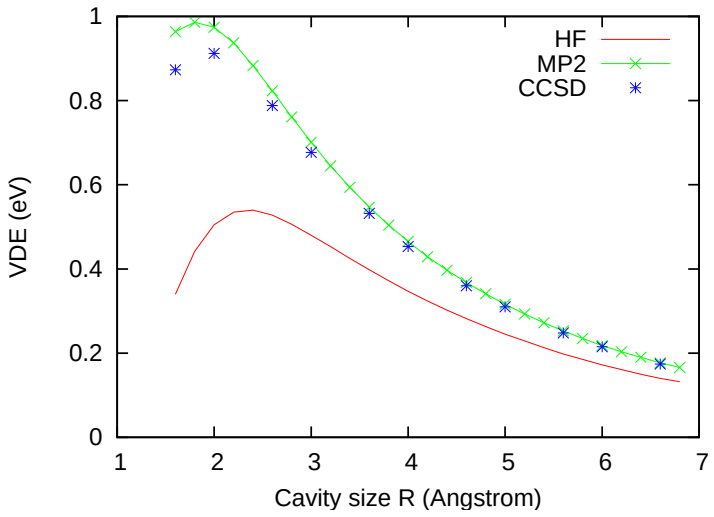

FIG. SI-8: Hartree-Fock and MP2 VDE (eV) vs. cavity radius R (Angstrom) for the $(H_2O)_6^-$ Kevan structure of Figure 8.

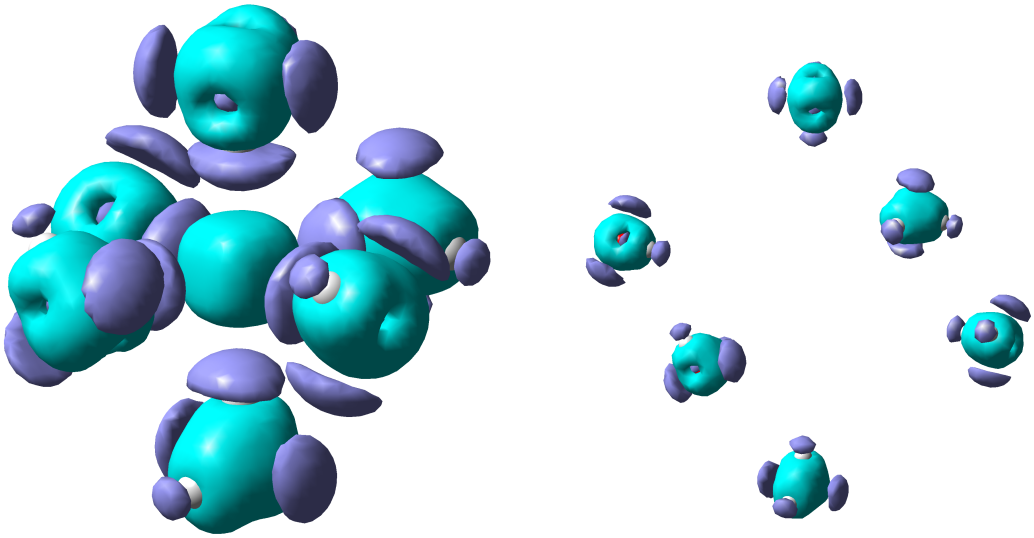

FIG. SI-9: Isosurfaces $|\Delta\rho(\vec{r})| = 0.001$ bohr^{-3} of the difference between MP2 and Hartree-Fock electron densities for the Kevan structure at $R = 2.0$ Angstrom (left) and $R = 6.0$ Angstrom (right). Electron correlation populates the regions outside O-H bonds (dark blue) and depopulates the bonding regions and the small cavity's center (light blue).

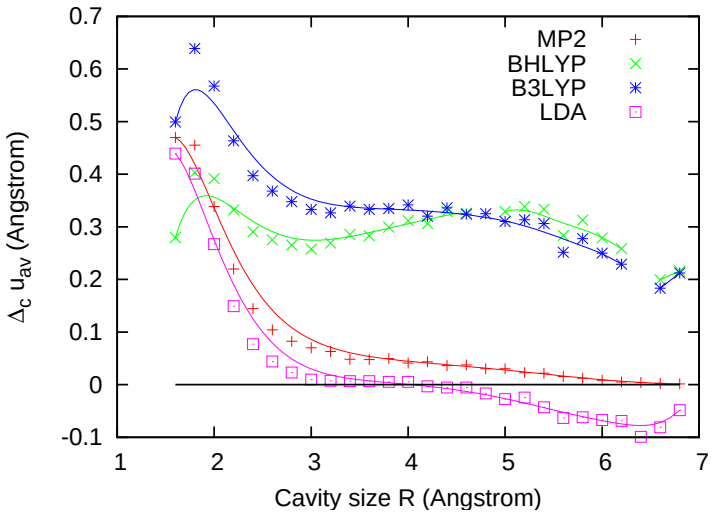

FIG. SI-10: MP2 and DFT $\Delta_c u_{av}$ (Angstrom) plotted vs. cavity radius R (Angstrom) for the Kevan structure of Figure 8.

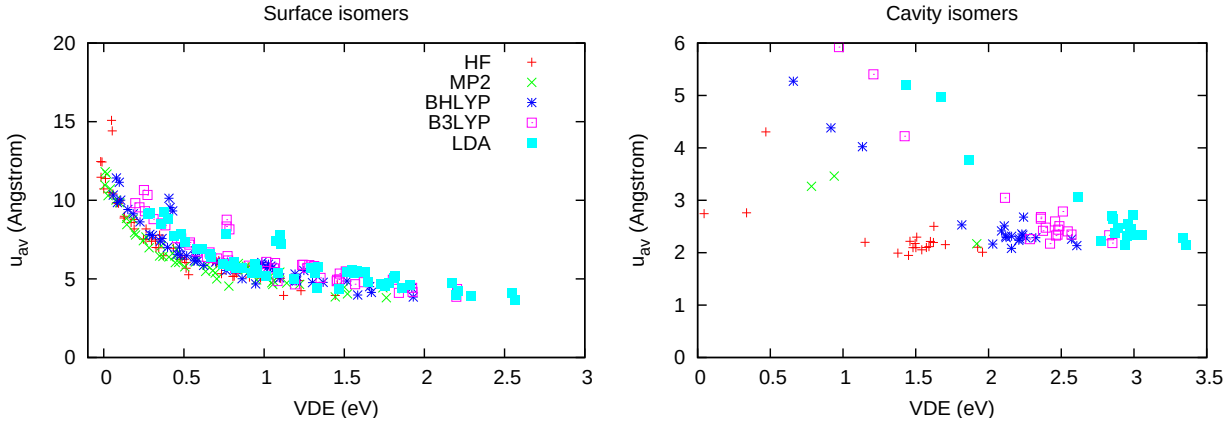

FIG. SI-11: Hartree-Fock, MP2, and DFT solvated electron delocalization u_{av}, plotted vs. the corresponding VDE, for surface and cavity states of $(H_2O)_n^-$.

SI-IV. AMMONIATED ELECTRONS

.

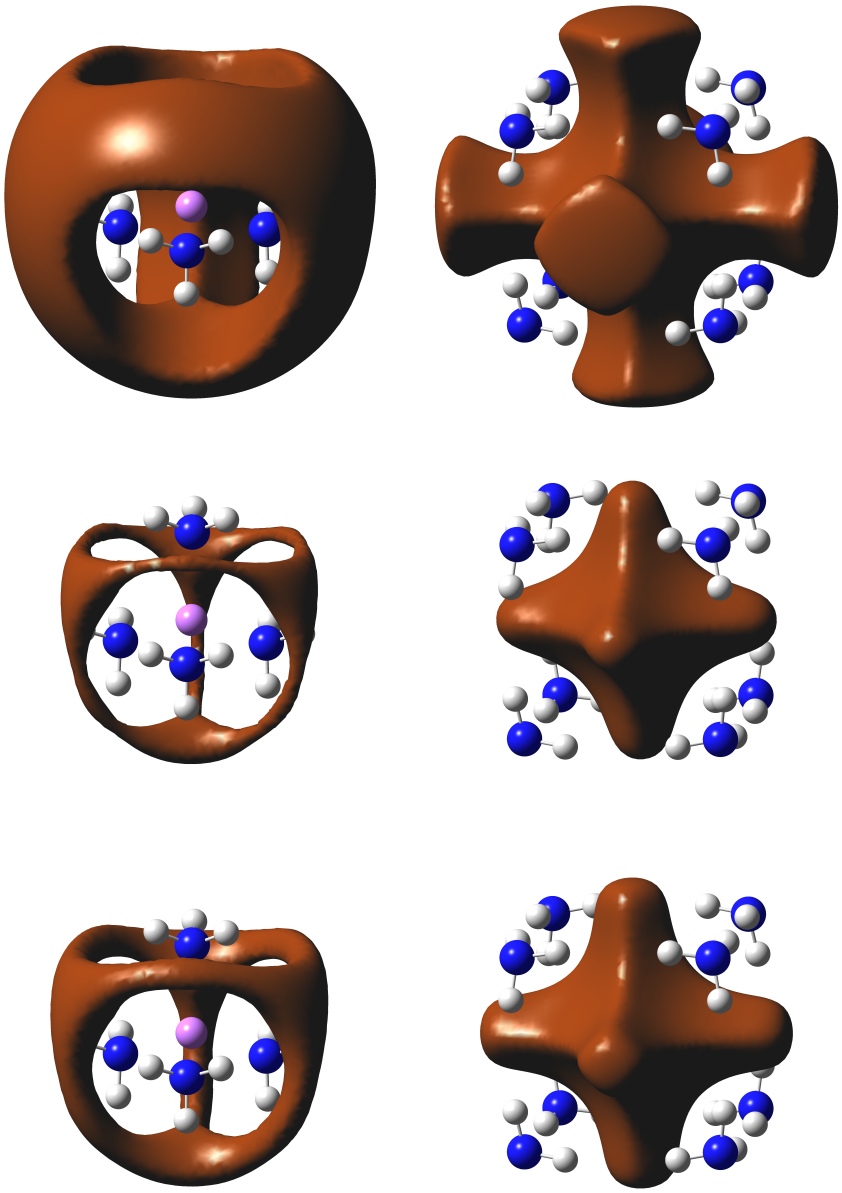

FIG. SI-12: Isosurfaces of the Hartree-Fock (top), LDA (middle), and B3LYP (bottom) EDR($r; u_{av}$) for the $Li(NH_3)_4$ (left) and $e^-@(NH_3)_8$ (right) of Figure 10.

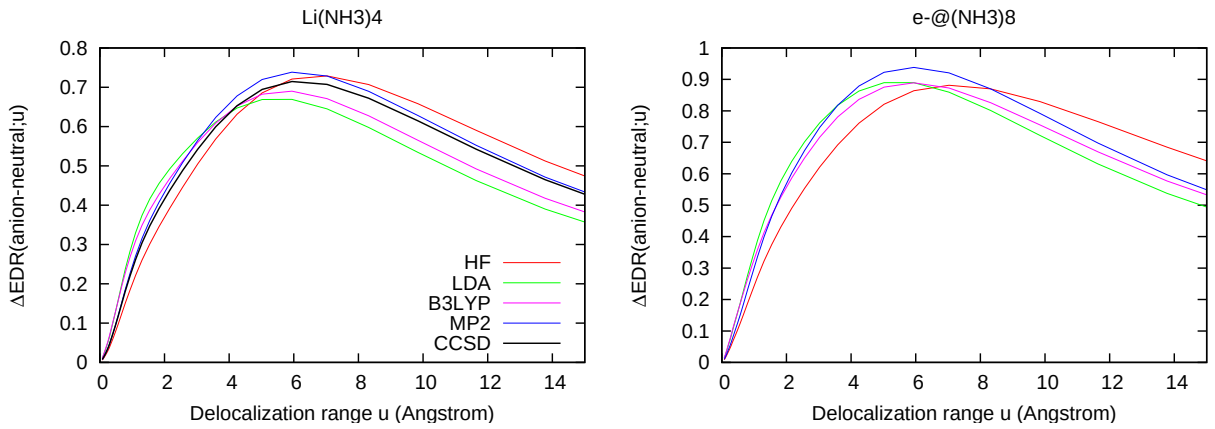

FIG. SI-13: ΔEDR(anion-neutral; u) for $Li(NH_3)_4$ and $e^-@(NH_3)_8$ of Figure 10.

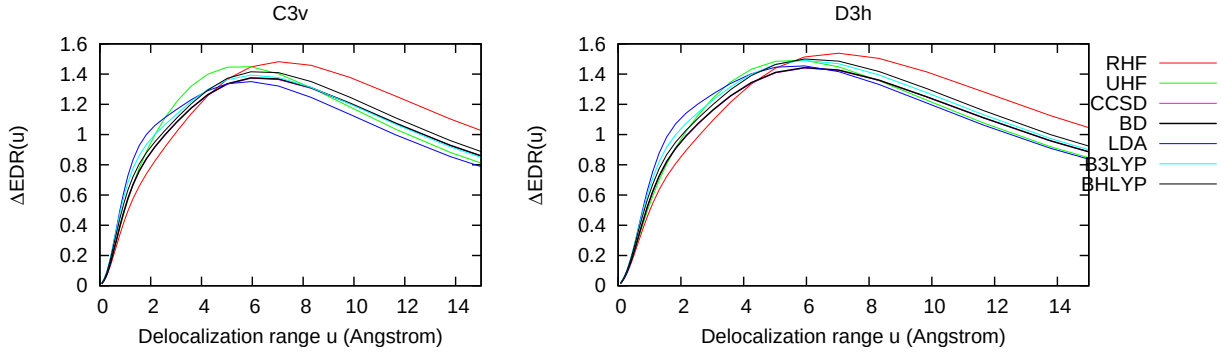

FIG. SI-14: ΔEDR(neutral-dication; u) for C_{3v} (left) and D_{3h} (right) isomers of singlet $(Li(NH_3)_4)_2$ of Figure **??**.

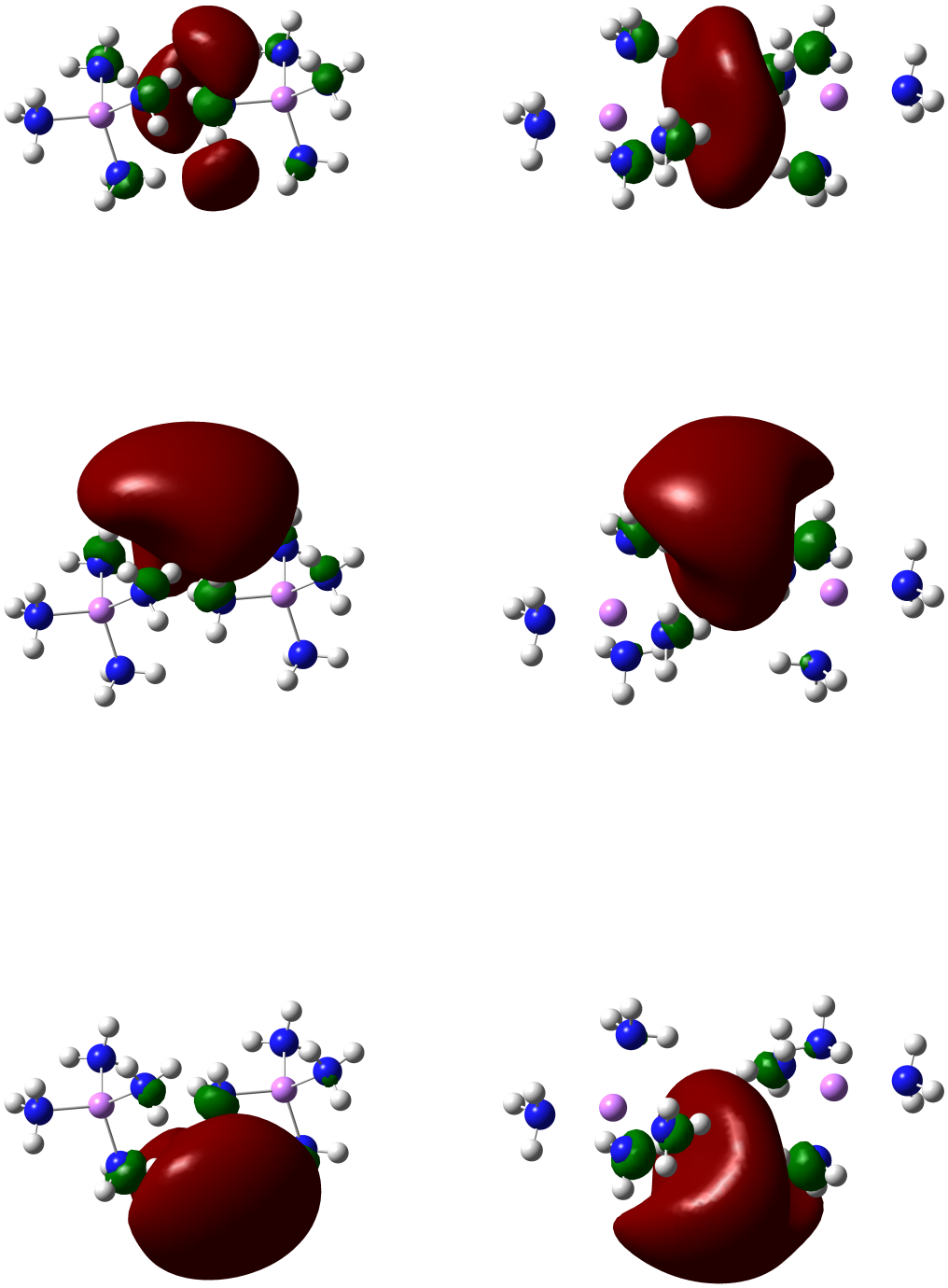

FIG. SI-15: Isosurfaces HOMO=0.02 bohr$^{-3/2}$ of the RHF (top), ↑-spin UHF (middle), and ↓-spin UHF (bottom) HOMO of C_{3v} (left) and D_{3h} (right) $(Li(NH_3)_4)_2$

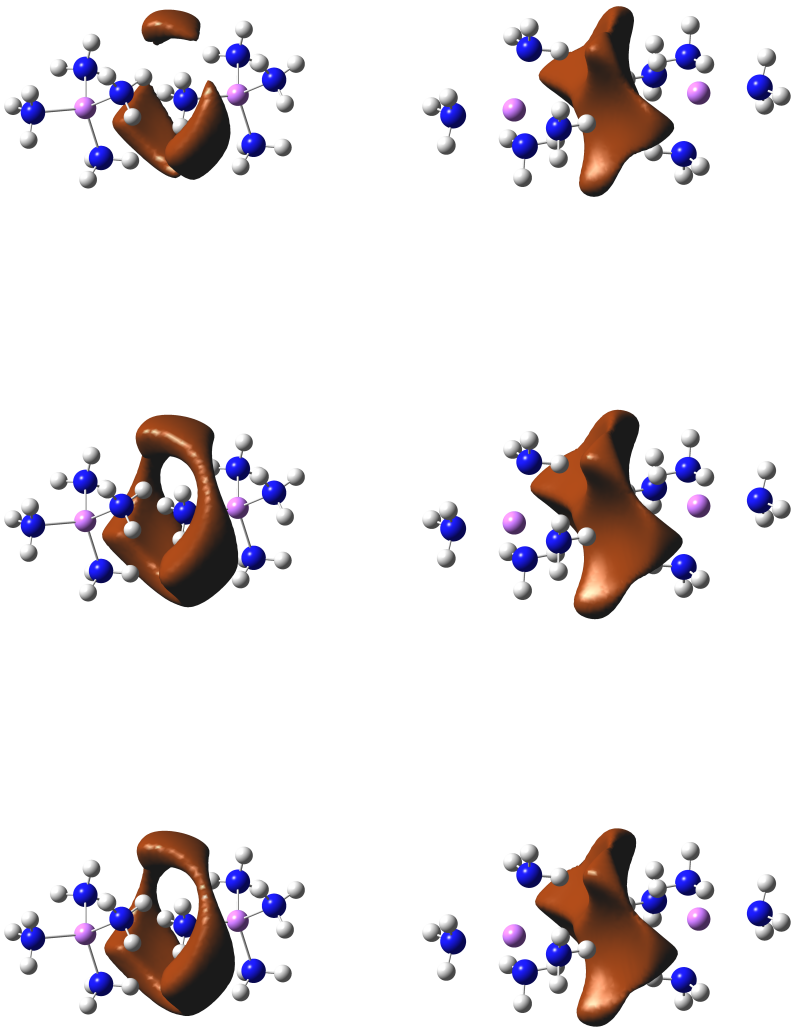

FIG. SI-16: Isosurfaces EDR($\vec{r}; u_{av}$)=0.7 of the LDA (top), B3LYP (middle), and CCSD (bottom) EDR, of C_{3v} (left) and D_{3h} (right) $(Li(NH_3)_4)_2$.

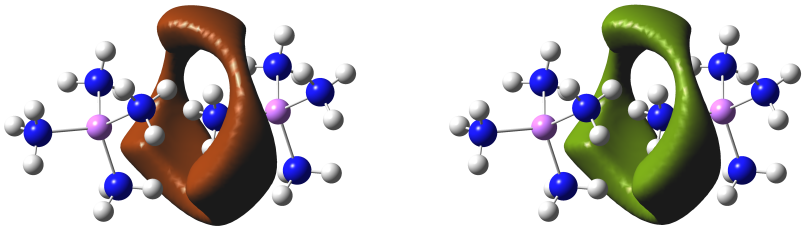

FIG. SI-17: Isosurfaces EDR($\vec{r}; u_{av}$)=0.7 of the ↑-spin (left) and ↓-spin (right) unrestricted Brückner doubles EDR of C_{3v} $(Li(NH_3)_4)_2$.

SI-V. TRANSITION TO A METALLIC STATE

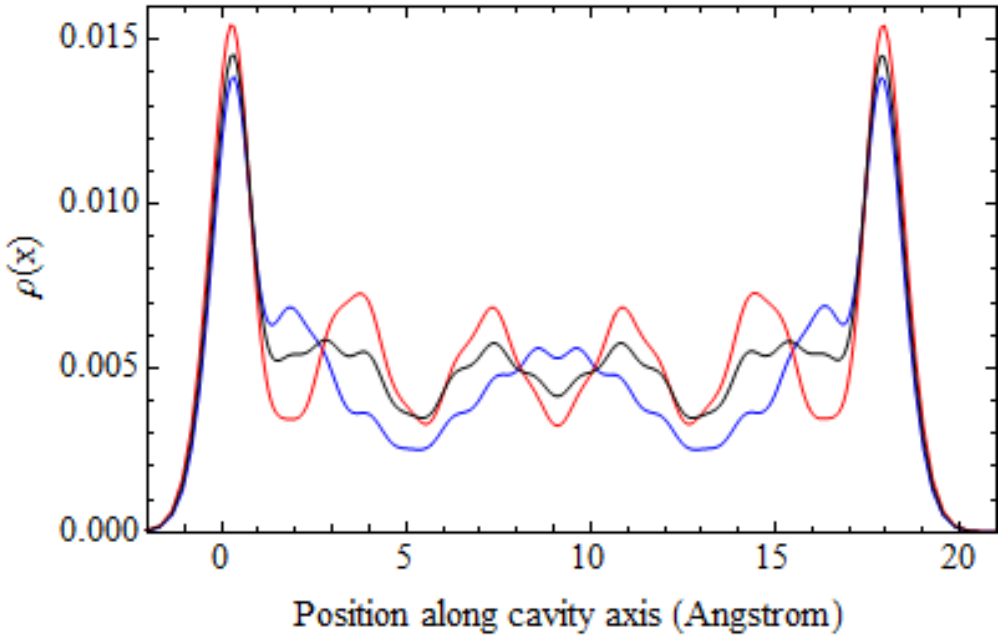

FIG. SI-18: Total electron densities $\rho(x)/2$ at points x along the cavity center for the cavity of Figure 13.

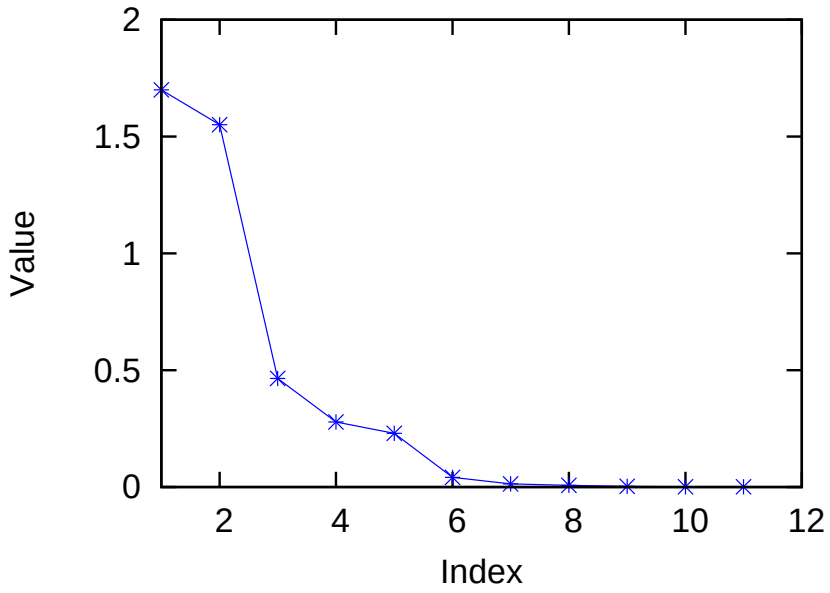

FIG. SI-19: Eigenvalues of the CASSCF(6,12) MO-basis one-particle density matrix for the cavity of Figure 13.